Bioresource Technology 417 (2025) 131856

Contents lists available at ScienceDirect

Bioresource Technology

journal homepage: www.elsevier.com/locate/biortech

Distinct lignocelluloses of plant evolution are optimally selective for complete biomass saccharification and upgrading Cd^{2+}/Pb^{2+} and dye adsorption via desired biosorbent assembly

Huiyi Zhang [a,b,1], Yongtai Wang [a,b,1], Hao Peng [a,b], Boyang He [a,b], Yunong Li [a,b], Hailang Wang [a,b], Zhen Hu [b,c], Hua Yu [a], Yanting Wang [a], Mengzhou Zhou [a], Liangcai Peng [a,b], Miao Wang [a,*]

[a] Key Laboratory of Fermentation Engineering (Ministry of Education), Hubei Key Laboratory of Industrial Microbiology, Cooperative Innovation Center of Industrial Fermentation (Ministry of Education & Hubei Province), School of Life and Health Sciences, Hubei University of Technology, Wuhan, 430068, China
[b] College of Plant Science & Technology, Huazhong Agricultural University, Wuhan 430070, China
[c] Houji Laboratory of Shanxi Province, Academy of Agronomy, Shanxi Agricultural University, Taiyuan, China

HIGHLIGHTS

- Distinct lignocelluloses of plant evolution for varied biomass saccharification.
- Near-complete saccharification of desired lignocellulose for ethanol conversion.
- Selective lignocellulose as optimal biosorbent for the highest Cd/Pb adsorption.
- Specific biosorbent rich at cellulose nanofibrils for maximizing dye adsorption.
- A novel strategy for efficient bioethanol conversion or biosorbent assembly.

GRAPHICAL ABSTRACT

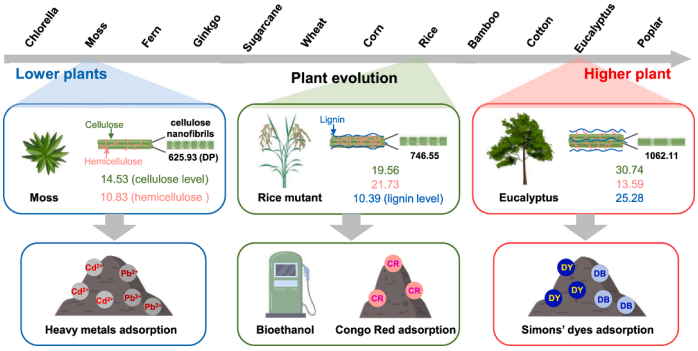

ARTICLE INFO

Keywords:
Wall polysaccharides
Cellulosic ethanol
Heavy metals
Dye removal
Oxidative catalysis

ABSTRACT

In this study, 15 plant species representing plant evolution were selected, and distinct lignocellulose compositions for largely varied biomass enzymatic saccharification were detected. By comparison, the acid-pretreated lignocellulose of rice mutant was of the highest Congo-red adsorption (298 mg/g) accounting for cellulose accessibility, leading to complete cellulose hydrolysis and high bioethanol production. By conducting oxidative-catalysis with the acid-pretreated lignocellulose of moss plant, the optimal biosorbent was generated with maximum Cd/Pb adsorption (54/118 mg/g), mainly due to half-reduced cellulose polymerization degree and raised functional groups accountable for multiple physical and chemical interactions. Furthermore, the acid-pretreated lignocellulose of eucalyptus was of large and small pores for much higher adsorption capacities with direct-yellow and direct-blue than those of the previously-reported. Therefore, this study raises a mechanism model about how distinct lignocelluloses of plant evolution are selective for complete biomass

* Corresponding author.
E-mail address: wanger726@163.com (M. Wang).
[1] The authors contributed equally.

https://doi.org/10.1016/j.biortech.2024.131856
Received 10 September 2024; Received in revised form 22 October 2024; Accepted 20 November 2024
Available online 22 November 2024

saccharification and optimal biosorbents assembly, providing insights into lignocellulose biosynthesis and biomass conversion.

1. Introduction

As traditional fossil energy sources are facing prominent shortage and excessive carbon liberation, it is imperative to develop various renewable energy as partial replacement of petrol fuels (Tan and Nielsen, 2022). Biomass-derived energy has thus emerged as a significant avenue for seizing energy crisis and environmental pollution (Park et al., 2023). Generally, plant cell walls provide the most abundant lignocelluloses convertible for biofuels and bioproducts (Su et al., 2024). However, as plant cell walls form a barrier for dynamic adaptation of various stresses, their recalcitrant property primarily decides a high-cost biomass saccharification and low-efficiency biofuel conversion (Zoghlami and Paës, 2019).

Plant cell walls are composed of cellulose, hemicellulose and lignin with small amounts of pectin and wall proteins. During biological evolution, plant species develop highly specific cell walls for diverse biological functions to maintain plant growth and development (Cosgrove, 2024). With increasing evolutionary advancement, lower plants are consequently emerged such as algae, mosses and gymnosperms, whereas angiosperms are undergoing extensive to give rise to a variety of morphological and ecological species including herbaceous crops and woody trees, thereby providing diverse biomass resources (Soltis et al., 2008; Wang and Ran, 2014). Nonetheless, as current research mainly focuses on the utilization of agricultural and forestry lignocelluloses (Sun et al., 2018; Wang, et al., 2021), little is explored about specific biomass applications from lower to higher plants.

As an excellent biofuel, cellulosic ethanol is typically produced through biochemical conversion of lignocellulosic biomass (Hu et al., 2023). However, lignocellulose recalcitrance requires extremely physical and chemical pretreatments and costly enzymatic hydrolyses along with potential secondary waste release (Huang et al., 2022). Alternatively, recalcitrance-reduced lignocellulose substrates are increasingly employed to achieve cost-effective biofuels and value-added bioproducts (Wang et al., 2024).

Over the past decade, adsorbent has gained widespread attention in wastewater treatment due to its simple and efficient characteristics. Although thousands of materials are able to prepare adsorbents, lignocellulose substrates are increasingly employed to generate biosorbents (Yaashikaa et al., 2021). Due to limited active sites of lignocelluloses, various modification methods are further performed to enhance adsorption capacity and efficiency (Hokkanen et al., 2016; Çelebi, 2020). However, it remains to explore the desirable lignocellulose applicable for maximizing adsorption capacity.

In this study, total 15 plant species from lower plants to higher ones were selected, and then their distinct lignocellulose compositions for varied biomass enzymatic saccharification were determined. Meanwhile, this study attempted to achieve near-complete saccharification towards the highest bioethanol production. The pretreated lignocelluloses were further employed to generate the desired biosorbents for maximum adsorption capacity. Finally, this study proposed a novel hypothetic model to address the following issues: (1) Whether the representative plant species could provide distinct lignocellulose substrates; (2) What is the desirable lignocellulose for near-complete biomass saccharification; (3) Why the optimal lignocelluloses are selectable for generations of high-performance biosorbents; (4) How a powerful strategy is applicable for efficient bioethanol productivity or effective exclusions of industry dyes and agriculture heavy metals.

2. Material and methods

2.1. Collection of biomass samples

The chlorella powder was purchased from Shengqing Biotechnology Co., Ltd, Xi'an, China, and the stem tissues of chlorella (*Chlorella vulgaris*), moss (*Hypnum plumaeforme*) and fern (*Adiantum capillus-veneris*) were obtained from Shangcheng County, Xinyang, China. The straws/stem tissues were collected from ginkgo (*Ginkgo biloba*), sugarcane cultivars (GT42), corn (Z31 and *bk1*), wheat (ZM9023 and ZT5), poplar (*Populus nigra*), rice cultivar (NPB) and its mutant (*snc11*) and cotton (KZ201) grown in experimental fields of Huazhong Agricultural University. The corn mutant (*bk1*) is identified as previously reported (Wu et al., 2019), and rice mutant (*snc11*) was obtained from site mutation of OsCESA7 with 3 bp deletion ($CTG_{1012\text{-}1014}$) of P-CR region by using CRISPR/Cas9 system as previously described (Hu et al., 2023). The stem tissues of eucalyptus (*Eucalyptus 3229*) were collected from Guangdong Eucalyptus Germplasm Field, Zhanjiang, China. The bamboo plants (*Phyllostachys edulis*) were planted in the experimental field of Zhejiang Agricultural University. All mature tissues were dried at 55 °C, cut into small pieces, screened by a 40-mesh sieve and stored in a dry container.

2.2. Wall polymers extraction and determination

Plant cell wall fractionation was accomplished as previously described (Zhang et al., 2023). The hexose, pentose and uronic acids assays were measured by UV–VIS spectrometer (V-1100D, Shanghai MAPADA Instruments Co.) (Yu et al., 2019). Total lignin was measured using a two-step acid hydrolysis method (Yuan et al., 2021).

2.3. Monosaccharides and cellulose feature assays

Monosaccharides of wall polysaccharides were determined by GC–MS (Shimadzu GCMS-QP2010 Plus) (Ai et al., 2024). Cellulose crystalline index (CrI) was detected by X-ray diffraction method (Hu et al., 2023). The degree of polymerization (DP) of cellulose was measured by the viscometry method (Fan et al., 2022).

2.4. Biomass pretreatment, enzymatic saccharification and yeast fermentation

The chemical (H_2SO_4) pretreatments were conducted as previously described (Gu et al., 2021). After pretreatment, the whole slurry was directly added for enzymatic hydrolysis containing 2.0 g/L mixed-cellulase enzymes (Imperial Jade Biotechnology Co., Ltd. Ningxia, China) with final concentrations of cellulases at 13.25 FPU g-1 biomass and xylanase at 8.4 U g-1 biomass with 3.3% (w/v) solid loading for 48 h in tubes as described (Zhang et al., 2023). Yeast *Saccharomyces cerevisiae* strain (purchased from Angel Yeast Co., Ltd., Yichang, China) was used in all fermentation reactions, and the yeast powder was dissolved in 0.2 M phosphate buffer (pH 4.8) for 30 min for activation prior to use. The yeast powder was suspended in pH 4.8 phosphate buffer to achieve in final concentration of 0.5 g/L in all fermentation tubes, and the fermentation was performed at 37°C for 48 h in tubes as described (Fan et al., 2022). The ethanol yield was estimated by $K_2Cr_2O_7$ method (Fan et al., 2022). All experiments were performed in independent triplicate.

2.5. Measurements of Simons' stain and Congo red adsorption

Simons' stain was performed to detect lignocellulose porosity (Kwok et al., 2017). Congo red (CR) stain was applied to detect cellulose

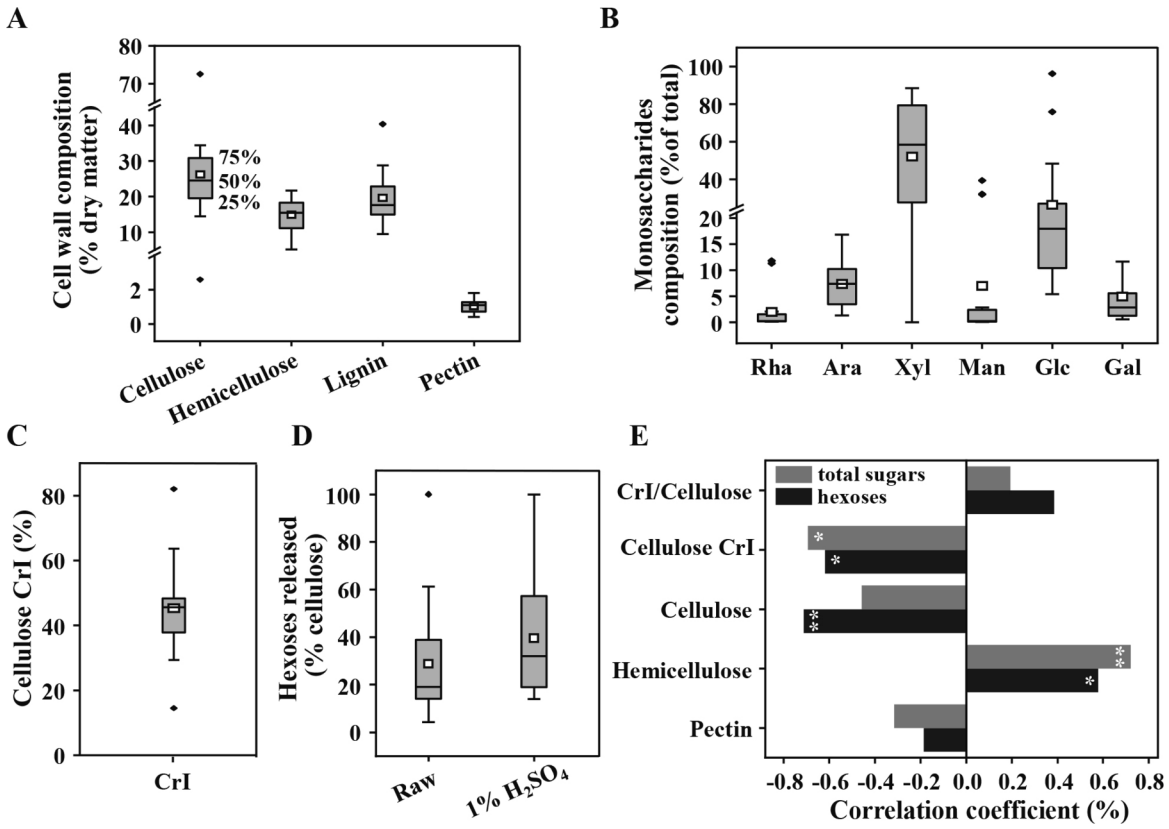

Fig. 1. Variation of lignocellulose compositions and features of plant evolution resources. (A) Cell wall components (n = 15, except lignin n = 12); (B) Monosaccharides composition (%) of non-cellulosic polysaccharides (n = 15); (C) Cellulose crystalline index (CrI) (%) (n = 15); (D) Hexoses yield (% cellulose) from enzymatic hydrolysis after 1% H_2SO_4 pretreatment or from direct hydrolysis of raw material/Raw (n = 15); (E) Correlation analysis between wall polymer levels (% dry matter) or cellulose CrI value and hexoses yields under 1% H_2SO_4 pretreatment (n = 15). The line and square within the box presented as the median and mean values of all data, the bottom and top edges of the box accountable for 25 and 75 percentiles of all data, and the bottom and top bars presented the maximum and minimum values of all data; * and ** as significant correlation at $p < 0.05$ and 0.01 levels, respectively.

accessibility (Wiman et al. 2012). All measurements were conducted at independent triplicate.

2.6. Adsorption of heavy metals

The lignocellulose residues were obtained as biosorbents samples from pretreatment and enzymatic hydrolysis after distilled water washing and drying at 50 °C. Batch adsorption experiments of $Cd(NO_3)_2$ and $Pb(NO_3)_2$ solutions were performed for 4.0 h at room temperature with 150 rpm shaking. The biomass loading is 1 g/L, and initial Cd^{2+} concentration Pb^{2+} concentration are 50 mg/L and 30 mg/L respectively. After reaction, the residual Cd^{2+} and Pb^{2+} levels were determined by flame atomic adsorption spectrophotometer (FAAS HITACHI Z-2000, Japan). All experiments were accomplished from independent triplicate.

The amount of adsorption at equilibrium q_e (mg/g) and the percentage removal efficiency (% R) were calculated (Vo et al., 2020). Langmuir isotherm and Freundlich isotherm models were characterized (Yang et al, 2020). The linear form of the pseudo-second-order equation was accomplished (Saman et al., 2018).

2.7. Two-step chemical modification of lignocellulose as high-performance biosorbent

The remaining residues (0.3 g) obtained from 1% H_2SO_4 pretreatment were incubated with 6 mL 1 % NaOH containing 0.9% H_2O_2 chemicals and shaken under 150 rpm for 2 h at 50 °C. After washing with distilled water, the residue was collected, dried at 50 °C, and stored as biosorbent sample for heavy metal adsorption assay. All experiments were accomplished from independent triplicate.

2.8. Characterization of biosorbents

The synthesized biosorbents were respectively characterized using Brunauer-Emmett-Teller (BET), X-ray photoelectron spectroscopy (XPS), scanning electron microscopy (SEM) and fourier transform infrared (FTIR) spectroscopy (Ramrakhiani et al., 2017; Huang et al., 2019).

2.9. Statistical analysis

Statistical analysis was completed using SPSS version 16.0 (Inc., Chicago, IL). Significant differences were conducted between two measurements by a two-tailed Student's *t*-test.

3. Results and discussion

3.1. Diverse lignocellulose substrates for varied biomass saccharification

As plant evolution drives diverse species to adapt various ecosystems, this study collected biomass samples of total 15 plant species representative from lower plants to higher ones, and then determined their cell wall compositions (Fig. 1). As a result, total 15 plant species are of largely varied cellulose, hemicellulose, lignin and pectic levels on a dry matter basis (Fig. 1A). As a comparison, cellulose levels are ranged from 3% to 73% (% dry matter) with coefficient variation (CV) of 56% and lignin contents are varied from 9% to 40% with CV of 41%, whereas hemicelluloses and pectin levels showed relatively less variations (see supplementary material). Particularly, total 15 plant species exhibited even more variations of major monosaccharides relative to their wall

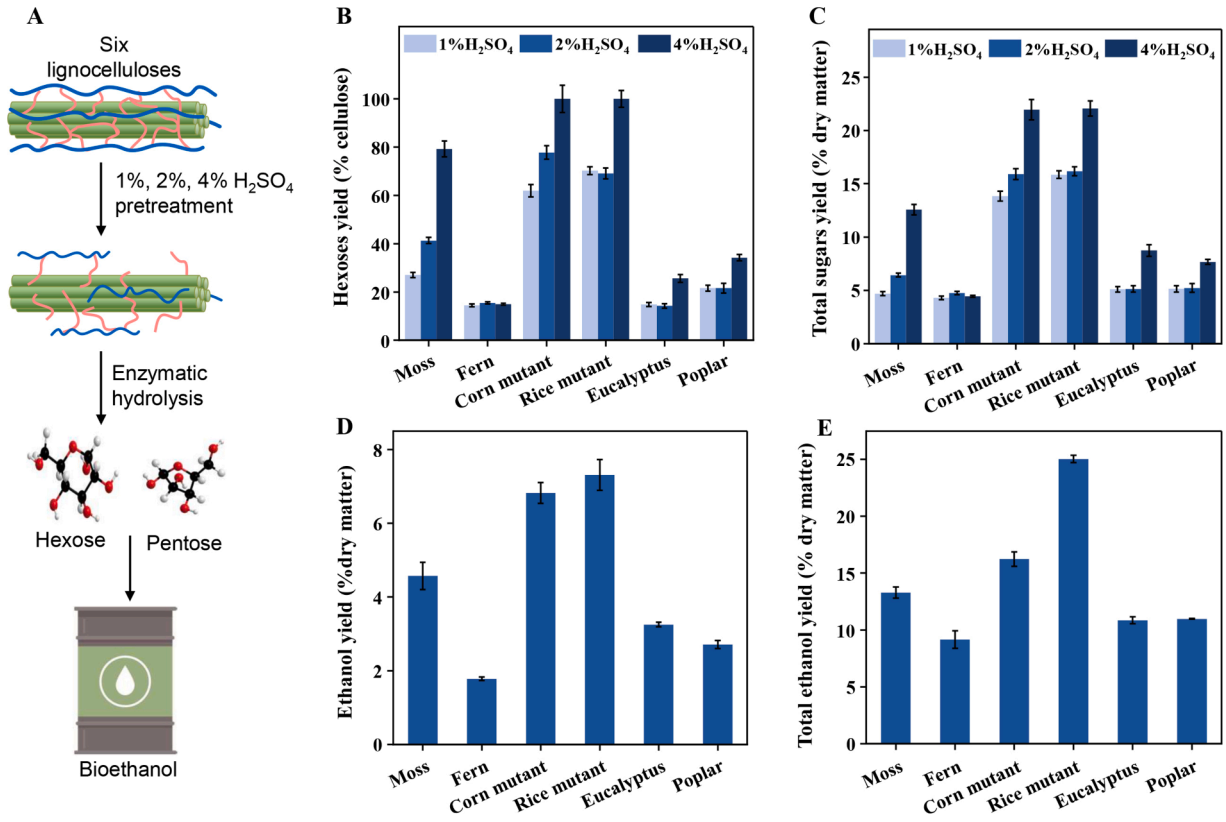

Fig. 2. Hexoses and bioethanol yields from enzymatic hydrolyses of six plant species after H_2SO_4 pretreatment at different concentrations. (A) Experimental flow chart for biomass saccharification and bioethanol fermentation; (B) Hexoses yield; (C) Total sugars (hexoses and pentoses) yield from enzymatic hydrolysis after pretreatment; (D) Ethanol yield by real yeast fermentation with hexoses released from enzymatic hydrolysis after 4% H_2SO_4 pretreatment; (E) Total ethanol yield by yeast fermentation with total sugars released from both enzymatic hydrolysis and 4% H_2SO_4 pretreatment with xylose-ethanol conversion in theory; Bar as means ± SD (n = 3).

polysaccharides (Fig. 1B). As cellulose crystallinity is a key feature (Ai et al., 2024), this work also determined varied cellulose crystalline index (CrI) values with CV of 33% (Fig. 1C). Hence, the diverse wall polymer levels/compositions and features should reflect plant dynamic adaptations to varied environments during plant evolution (Soltis et al., 2008; Wang and Ran, 2014).

Furthermore, this study performed direct enzymatic hydrolysis of raw biomass of 15 plant species, and determined their hexoses yields (% cellulose) from 4% to 100% or total sugars (hexoses and pentoses) yields (% dry matter) from 2% to 14% (Fig. 1D; see supplementary material). The Chlorella plant showed a complete biomass saccharification with hexoses yield of 100 %, due to its much lower cellulose level examined. Despite acid pretreatment could enhance sequential biomass saccharification (Zhang et al., 2021), this study detected steadily varied hexoses and total sugars yields, confirming their distinct lignocellulose compositions and features. Notably, the rice site-mutant was of the highest hexoses and total sugars yields among all sampled examined, being consistent with other OsCESAs site-mutans as previously reported (Hu et al., 2023). In addition, classic correlation analysis was performed between lignocellulose compositions/features and hexoses/total sugars yields of 15 plant species (Fig. 1E). Significantly, the cellulose levels and CrI values are examined as the negative factors accounting for hexoses and total sugars yields, whereas the hemicellulose contents positively affected biomass saccharification, in agreement with the previous findings (Leu and Zhu, 2013; Hu et al., 2023). As cellulose crystallinity is an integrative parameter accounting for cellulose nanofibrils assembly and cellulose microfibrils interaction with hemicellulose and lignin (Ai et al., 2024), which are major lignocellulose recalcitrant factors (Wang et al., 2024), total 15 plant species should be sufficient to represent diverse lignocellulose sources for largely varied lignocellulose recalcitrance and biomass enzymatic saccharification.

3.2. *Biochemical conversions of distinct lignocelluloses for high-yield bioethanol*

As total 15 plant species exhibited largely varied biomass saccharification, this study further performed H_2SO_4 pretreatments at three concentrations with six representative plant species (Fig. 2A). By comparison, the corn and rice mutants respectively showed nearly complete biomass saccharification with hexoses yields of 100% (% cellulose) and total sugars yields of 22% (% dry matter) under 4% H_2SO_4 pretreatment, whereas the fern and two woody trees had much lower hexoses (15%-34%) and total sugars (4%-8%) yields (Fig. 2B-C). Meanwhile, the moss plant remained incomplete cellulose hydrolysis with hexoses yield of 79% even upon 4% H_2SO_4 pretreatment, mainly due to its much high cellulose CrI value (see supplementary material). Despite all plant species showed a rising saccharification under higher H_2SO_4 concentrations, the two crop mutants maintained much more increased hexoses and total sugars yields, which should be due to their reduced lignocellulose recalcitrance as previously reported (Leu and Zhu, 2013; Wu et al., 2019; Hu et al., 2023).

Furthermore, this study conducted a classic yeast fermentation with enzymatic hydrates of six plant species after 4% H_2SO_4 pretreatments to achieve different bioethanol yields (Fig. 2D), consistent with their varied hexoses yields examined above. Despite of a similar hexoses yield, the rice mutant produced relatively higher bioethanol yield than the corn mutant did, probably due to less toxic compounds release that inhibit yeast fermentation in rice mutant (Wu et al., 2018). Notably, while all xylose was calculated for ethanol conversion in theory (Wu et al., 2019), the rice mutant could even produce much more total

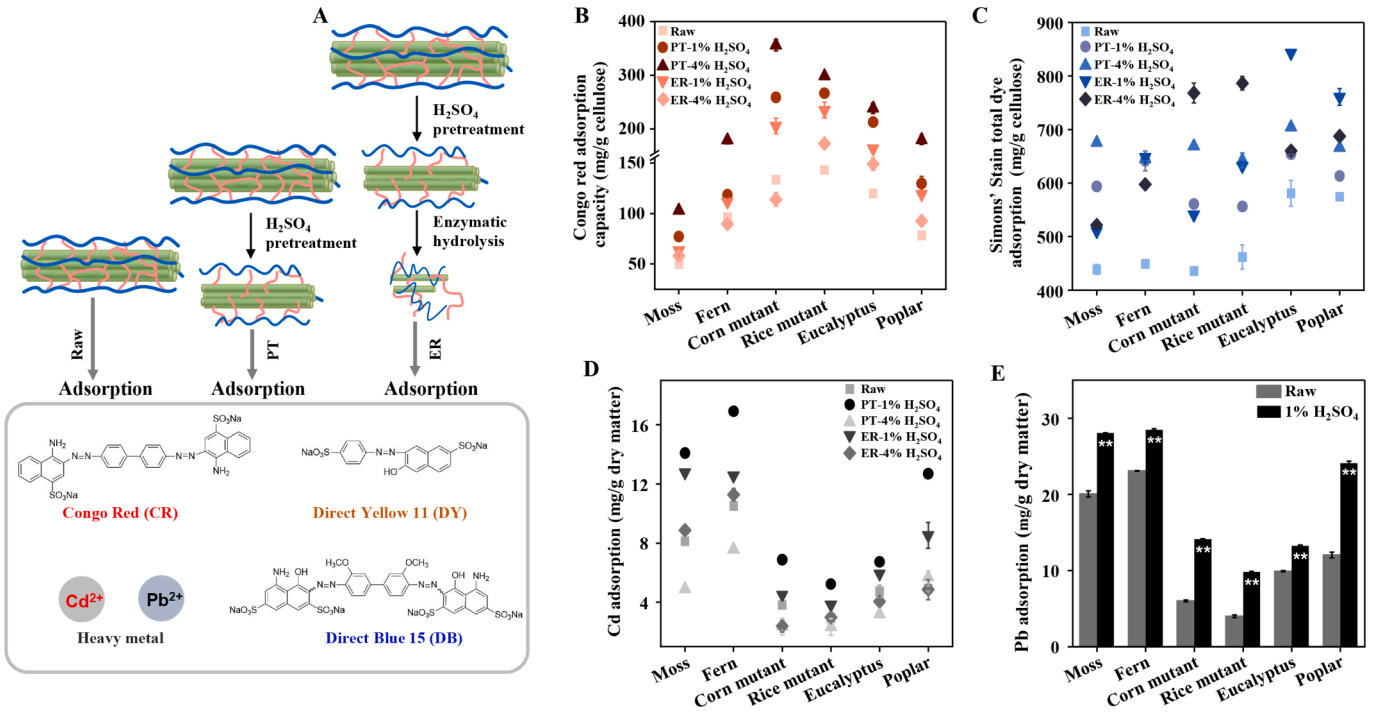

Fig. 3. Acid-pretreated lignocelluloses of six plant species as the biosorbents for absorptions with three organic dyes and two heavy metals. (A) Experimental flow chart; (B) Congo-red stain adsorption capacity; (C) Simons' Stain total dye (direct yellow/DY + direct blue/DB) adsorption capacity; (D) Cd adsorption capacity; (E) Pb adsorption capacity; Raw as raw biomass of plant species; PT-1% H_2SO_4 and PT-4% H_2SO_4 refer to 1% H_2SO_4 and 4% H_2SO_4 pretreated residues; ER-1% H_2SO_4 and ER-4% H_2SO_4 refer to enzyme-undigestible residues after 1% H_2SO_4 and 4% H_2SO_4 pretreatments, respectively; Bar as means ± SD (n = 3); ** As significant difference relative to the Raw (raw material) at $p < 0.01$ level by *t*-test (n = 3).

ethanol yield than other plant species (Fig. 2E), which should be owing to its complete cellulose hydrolysis, more soluble sugars accumulation and relatively higher hemicellulose deposition as previously examined in other similar site mutants of OsCESAs (Hu et al., 2023). Therefore, such distinct lignocellulose substrates of six plant species should be accountable for large variations of biomass saccharification and bioethanol conversion.

3.3. *Desirable biosorbents selective for organic dyes and heavy metals adsorptions*

Because six plant species provide distinct lignocellulose substrates, this study attempted to test their applications as biosorbents for relatively low-costly and high-effective adsorptions of three organic dyes and two heavy metals (Fig. 3). To find out the optimal biosorbents, this study explored five lignocellulose sources such as raw straw, two acid-pretreated lignocelluloses, and two enzyme-undigested residues of pretreated-lignocelluloses (Fig. 3A). As the CR is a major industry dye, its adsorption capacities with all lignocellulose samples of six plant species were examined (Fig. 3B). As a comparison, the 1% H_2SO_4-pretreated and 4% H_2SO_4-pretreated lignocelluloses showed the average CR adsorption capacities at 177 mg/g and 226 mg/g, whereas the raw biomass and enzyme-undigestible residues had the average CR adsorptions ranged from 104 mg/g to 150 mg/g (Fig. 3B). On the other hands, the corn and rice mutants exhibited much higher CR adsorption capacities (214 mg/g and 223 mg/g) than those of other four plant species (from 70 mg/g to 176 mg/g) in all five lignocellulose sources. Since CR staining is broadly applied to detect cellulose accessibility (Wiman et al., 2012), the acid-pretreated lignocelluloses of both corn and rice mutants should be of sufficiently accessible cellulose microfibrils as previously reported (Leu and Zhu, 2013; Wu et al., 2019), which could be employed as the desirable biosorbents for CR adsorption.

Since Simons' stain is a semi-quantitative assay for the porous volumes of accessible lignocellulosic substrates by using Direct Yellow 11 (DY) and Direct Blue 15 (DB) (Meng et al., 2015), this study also detected these two dyes adsorptions with all lignocellulose samples. As DY and DB dyes are accounting for relatively large and small pore sizes (Kwok et al., 2017), this study measured generally varied adsorption capacities of total (DY + DB) dyes among all lignocellulose substrates (Fig. 3C). Excepting the raw materials showing low adsorption capacities with DY and DB at 279 mg/g and 212 mg/g, the acid-pretreated lignocelluloses and enzyme-undigested residues were of much higher adsorption capacities such as average DY (315–343 mg/g) and DB (289–351 mg/g). Moreover, the lignocellulose substrate of eucalyptus plant consistently maintained the highest DY and DB adsorption capacities (Fig. 3C), suggesting that the woody species could generate the desirable biosorbents for efficient DY and DB adsorptions.

Moreover, this study employed all lignocelluloses substrates to test their adsorption capacities with Cd, a toxic heavy metal polluted in agricultural soil and daily location (Fig. 3D). In general, the 1% H_2SO_4-pretreated lignocelluloses and sequential enzyme-undigestible residues of all six plant species showed consistently high Cd adsorption capacities. In particular, two lower plants (moss, fern) remained the highest Cd adsorption capacities among all lignocellulose sources (Fig. 3D), which may mainly be owing to their rich pectin and hemicellulose proportions. As an exception, the raw materials of six plant species even had a slightly higher Cd adsorption value on average than those of the 4% H_2SO_4-pretreated lignocelluloses and sequential enzyme-undigestible residues, suggesting that the H_2SO_4 pretreatment at high concentration may remove active chemical groups of lignocellulose associated with Cd adsorption (He et al., 2021). In addition, this study utilized raw materials and 1% H_2SO_4-pretreated lignocelluloses to detect adsorption capacities with Pb, another major toxic heavy metal (Dubey et al., 2018). Likewise, two lower plants maintained consistently higher Pb adsorption capacities than those of other four plant species (Fig. 3E), which revealed that the moss and fern species could provide desirable biosorbents for heavy metals removals. Taken together, the 1% H_2SO_4-pretreated lignocelluloses substrates have mostly showed much

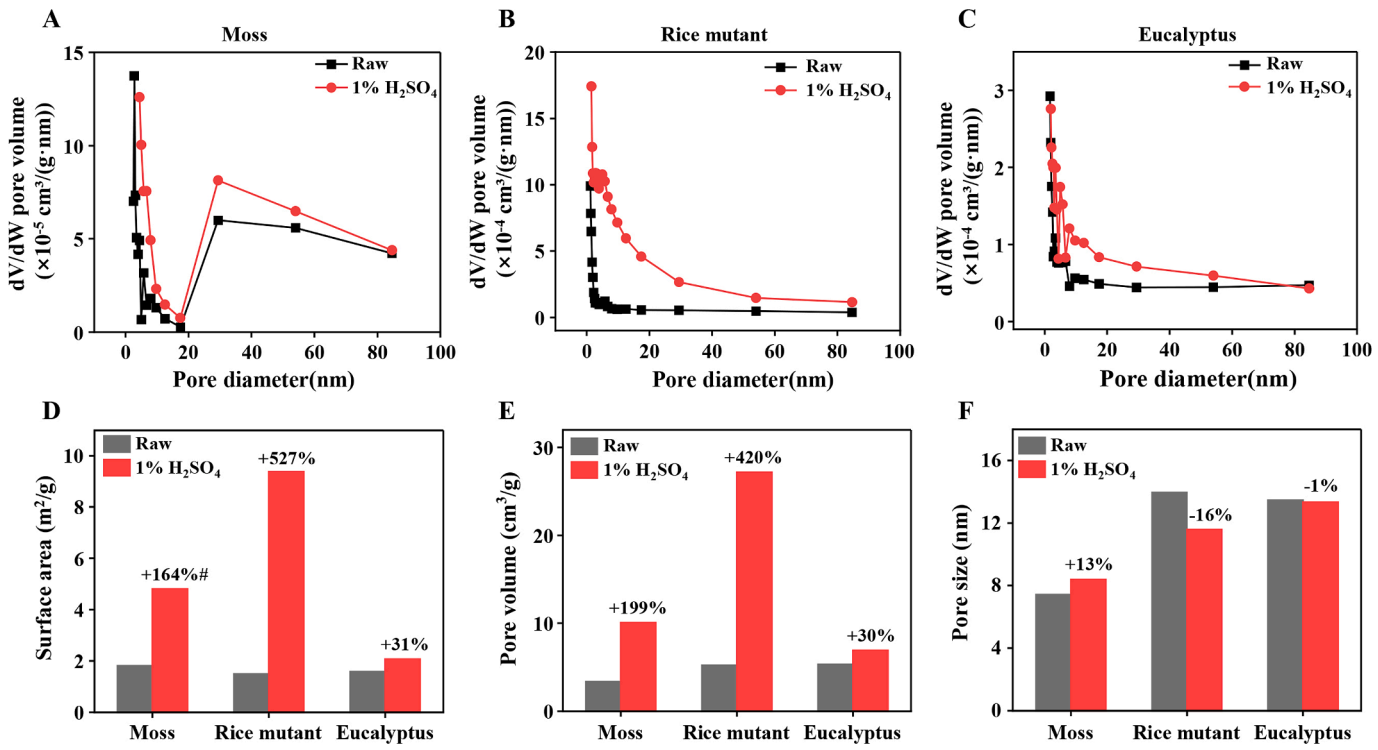

Fig. 4. Brunauer-Emmett-Teller (BET) analysis of lignocellulose porosity of three representative plant species after 1% H_2SO_4 pretreatment. (A-C) Barret-Joyner-Halenda (BJH) adsorption micropore distribution; (D) BET surface area; (E) Pore volume; (F) Pore size; # As increased (+) or decreased (−) percentage of the acid-pretreated lignocellulose relative to its raw material.

enhanced adsorptive efficiencies with three dyes and two heavy metals, but each type of plant species has its unique advantage for the highest adsorptive capacities.

3.4. Characterization of desired biosorbents in three representative plant species

Given that three types of plant species (moss, rice mutant, eucalyptus) could produce distinct lignocelluloses as unique biosorbents, this study further detect their porosity by performing classic BET assay (Fig. 4). Based on pore distribution profiling (Fig. 4A-C), the acid-pretreated lignocelluloses showed much improved specific surface area, pore volume and pore size, compared to their raw materials (Fig. 4D-F), which should be generally accountable for their remarkably raised adsorption capacities examined above. In particular, the acid-pretreated lignocellulose of rice mutant exhibited much larger surface area and more pore volume than the moss and eucalyptus did (Fig. 4D, E), interpreting why the rice mutant was of the highest CR adsorption capacity examined. On the other hand, the acid-pretreated lignocellulose of eucalyptus showed relatively larger pore size on average than the moss and rice mutant did (Fig. 4F), which should be a major cause about the highest DY and DB adsorption capacities examined in two woody trees.

By performing FTIR scanning, chemical group alteration in three representative plant species was observed (see supplementary material). Compared to their raw materials, the acid-pretreated lignocelluloses exhibited multiple characteristic peaks altered for corresponding to functional groups (see supplementary material), revealing that acid-pretreatment could partially digest hemicellulose (1053 cm^{-1}, 1371 cm^{-1}) and pectin (1631/1640 cm^{-1}) with co-extraction of lignin (1231 cm^{-1}, 1512 cm^{-1}, 1735 cm^{-1}). In terms of more chemical group alteration in the rice mutant, effective lignocellulose destruction should occur from acid pretreatment enabled for its near complete cellulose digestion and highest cellulose accessibility examined above. Under

Table 1
Cellulose degree of polymerization (DP) before and after 1% H_2SO_4 pretreatment.

Sample	Raw material	1 % H_2SO_4 pretreated lignocellulose
Moss	625.93 ± 2.65	309.81 ± 0.00** (−50 %) #
Fern	900.57 ± 2.16	640.56 ± 0.00** (−29 %)
Corn mutant	891.64 ± 0.00	683.26 ± 1.40** (−23 %)
Rice mutant	746.55 ± 0.93	691.94 ± 7.37** (−7%)
Eucalyptus	1062.11 ± 3.03	582.95 ± 1.23** (−45 %)
Poplar	958.05 ± 8.40	831.82 ± 2.75** (−13 %)

** As significant difference between the raw material and lignocellulose by *t*-test at $p < 0.01$ levels (n = 3);
# As reduced percentage of lignocellulose DP value relative to raw material; Data as means ± SD (n = 3).

SEM observation, the acid-pretreated lignocelluloses exhibited much rougher faces than those of their raw materials, but moss sample was of much smaller grain-like structure (see supplementary material), which should be assembled from its relatively higher proportions of hemicellulose and pectin and less cellulose microfibrils with a low degree of polymerization (310 DP) (Table 1). By comparison, the rice mutant and eucalyptus samples exhibited relatively smooth and large grain structures, mainly due to their partial lignin assembly and longer cellulose microfibrils deposition (583-832 DP). Because hemicellulose and pectin are rich at active chemical groups, it may explain much higher Cd/Pb adsorption capacities examined in two lower plant species.

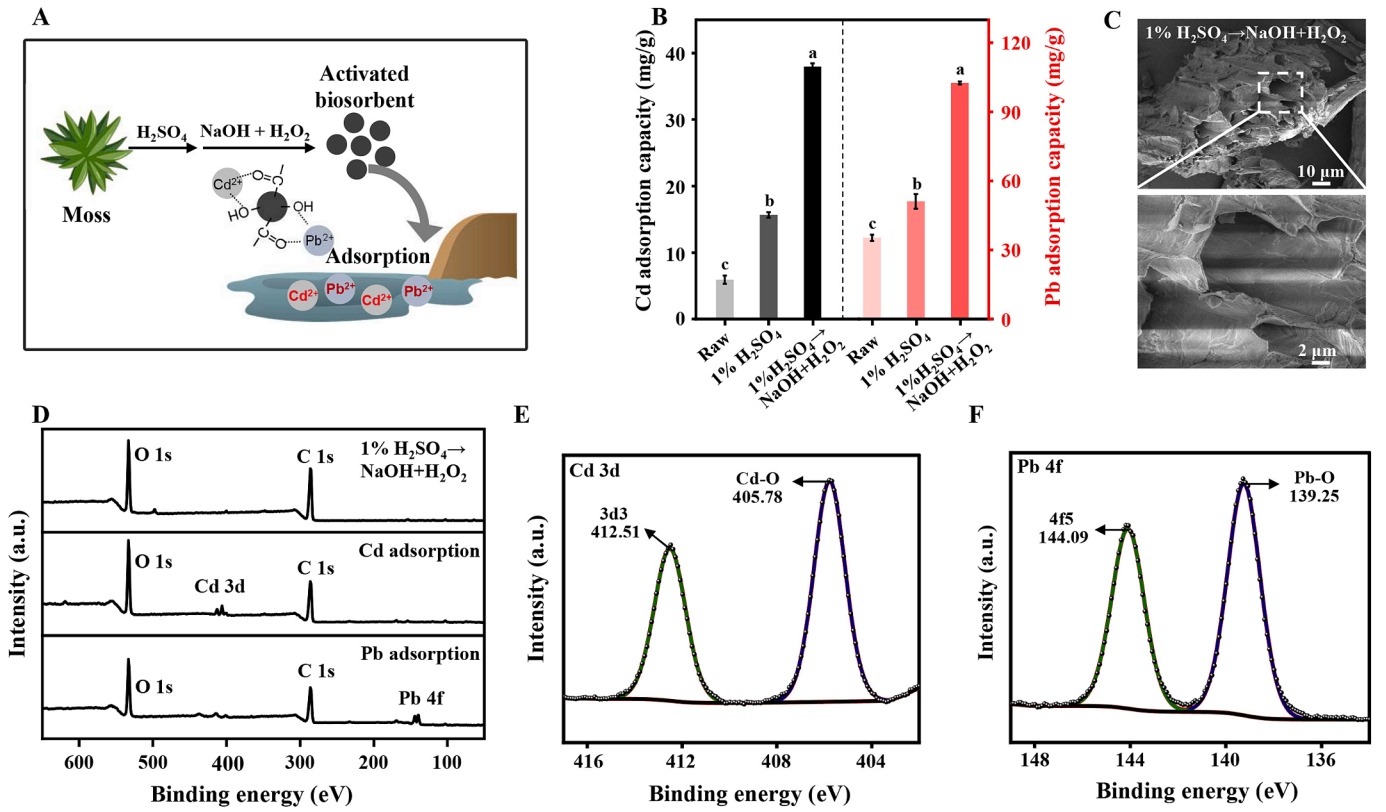

Fig. 5. Characterization of two-step chemical-modified biosorbent of moss plant as biosorbent for heavy metals adsorption. (A) Experimental flow chart; (B) Cd and Pb adsorption capacities of two-step chemical (1% H_2SO_4 → NaOH + H_2O_2) modified biosorbent relative to the raw material and one-step acid-pretreated lignocellulose; (C) Scanning electron microscopy (SEM) observation of biosorbent surfaces; (D) X-ray photoelectron spectroscopy (XPS) spectrum profiling of biosorbent before and after Cd/Pb adsorption; (E) XPS of Cd 3d spectrum for Cd adsorption. (F) XPS of Pb 4f spectrum for Pb adsorption.

3.5. Integrated chemical modification to maximize heavy metal adsorption

Although the lower plant species were of relatively higher Cd/Pb adsorption capacities, they appeared to be slightly lower compared to the optimal biosorbents as previously generated from other biomass resources (Abdolali et al., 2017; González-Feijoo et al., 2024). Hence, this study used well-mixed chemicals (NaOH, H_2O_2) to incubate with the acid-pretreated lignocellulose of moss plant to modify biosorbent by oxidative reaction (Fig. 5A). As comparison with the one-step acid-pretreated lignocellulose, this two-step oxidative-modified biosorbent showed significantly increased adsorption capacities with Cd and Pb by 2.4- and 2.0-folds, respectively (Fig. 5B). Under SEM observation, the two-step modified biosorbent exhibited a typical micro- and nano-scale biosorbent assembly with a regular porous structure (Fig. 5C), which was obviously different from the one-step acid-pretreated lignocellulose observed (see supplementary material). Such porous biosorbent construction should maintain a high porosity favor for physical interaction with heavy metals (Wu et al., 2022). By performing X-ray photoelectron spectroscopy (XPS) analysis with two-step modified biosorbent, two typical peaks corresponding for Cd 3d and Pb 4f (398 eV-417 eV and 134 eV-149 eV) were observed, indicating chemical interactions between the biosorbent and Cd^{2+} and Pb^{2+} ions (Fig. 5D). The peaks for C-C, C-O-C, and O-C=O in C 1 s, and peaks for C=O and C-O in O 1 s, and the Cd 3d and Pb 4f are respectively accounting for the formations of Cd-O and Pb-O bonds (Fig. 5E, F; see supplementary material). Based on three typical C-linkages and two typical O-linkages analyses, the two-step modified biosorbent showed a decrease of C-C/C=O proportion with relatively increased C-O after Cd^{2+} and Pb^{2+} adsorptions, suggesting that the -COOH and -OH groups of biosorbent should involve in chemical interactions with heavy metals (see supplementary material). Hence, the two-step modified lignocellulose of moss plant should be of an optimal biosorbent assembly from more active chemical modification occurrences.

3.6. Characteristic Cd/Pb adsorptive models for optimal biosorbents

To understand the two-step chemical-modified biosorbent of moss plant with much higher Cd/Pb adsorption capacity, this study further conducted classic adsorption experiments by supplying different dosages of heavy metals under a time course incubation (see supplementary material). As the initial concentrations of Cd and Pb are rising until being saturated, the two-step modified biosorbent maintained consistently higher adsorption capacities and efficiencies, compared to the

Table 2
Langmuir and Fruendlich isotherm model for Cd/Pb adsorptions with two biosorbents of moss plant.

	Sample	Langmuir			Freundlich		
		q_{max}(mg/g)	b(L/mg)	R^2	K_F	n	R^2
Cd	1 % H_2SO_4	14.33	2.17	0.9993	7.37	3.90	0.6621
	1 % H_2SO_4 → NaOH + H_2O_2	53.76	0.98	0.9906	27.05	4.50	0.8865
Pb	1 % H_2SO_4	41.32	1.07	0.9996	26.27	8.40	0.8376
	1 % H_2SO_4 → NaOH + H_2O_2	117.68	0.36	0.9988	62.99	7.00	0.9441

Table 3
Kinetic parameters of the pseudo-second-order equation for Cd/Pb adsorptions with two biosorbents of moss plant.

	Sample	Experimental value	Kinetic parameters		
		q_e(mg/g)	K_2(g/min·mg)	q_e(mg/g)	R^2
Cd	1 % H_2SO_4	13.46	0.08	13.50	0.9998
	1 % H_2SO_4 → NaOH + H_2O_2	23.71	0.13	23.70	0.9999
Pb	1 % H_2SO_4	44.08	0.03	44.25	0.9999
	1 % H_2SO_4 → NaOH + H_2O_2	118.71	0.05	119.05	0.9995

one-step acid-pretreated lignocellulose (see supplementary material), which confirmed much enhanced Cd and Pb adsorption capacities in the two-step modified biosorbent (Fig. 5B). From the initial incubation with Cd and Pb for 10 mins, the modified biosorbent immediately showed much higher adsorption capacity and efficiency than those of the acid-pretreated lignocellulose by 3.8- and 2.8-folds (see supplementary material). During sequential long-time incubation, the modified biosorbent preserved consistently higher Cd/Pb adsorption, and reached to adsorption saturation at 60 min as reaction equilibrium. Further performing Langmuir and Freundlich modeling, both acid-pretreated lignocellulose and modified biosorbent were of extremely high R^2 values at > 0.99 from Langmuir equation, whereas the modified biosorbent remained higher values (0.88, 0.94) than the acid-pretreated lignocellulose did (0.66, 0.83) from Freundlich equation (Table 2). These findings thus revealed that both acid-pretreated lignocellulose and modified biosorbent mainly involve in single-layer chemical interaction with heavy metals due to extremely high R^2 values of Langmuir modeling, but the modified biosorbent should be more active for multiple-layer physical adsorption from its relatively higher R^2 value of Freundlich modeling (Sabarish and Unnikrishnan, 2018). Importantly, the pseudo-second-order dynamic modeling also showed extremely high R^2 values at > 0.999 for both acid-pretreated lignocellulose and modified biosorbent (Table 3), which further pointed out highly active chemical adsorptions with Cd and Pb (Sabarish and Unnikrishnan, 2018). Therefore, those models have confirmed that two-step chemical-modified biosorbent of moss plant could be applied as the optimal biosorbent for efficient heavy metal adsorption, due to extremely high chemical adsorption and active physical interaction.

3.7. *Mechanisms of high-yield biomass saccharification and high-performance biosorbent assembly*

Regarding all major findings achieved in this study referred with the previous reports, a hypothetic model was proposed to elucidate how distinct lignocelluloses of plant evolution are digestible and convertible for high bioethanol productivity and desired biosorbent assembly (Fig. 6). As a typical lower plant species, the moss plant consists of relatively high proportions of hemicellulose and pectin and small amount of low-DP cellulose with non-lignin deposition, which could effectively cause high-porosity lignocellulose formation with active chemical groups after 1% H_2SO_4 pretreatment was implemented for non-cellulosic polysaccharide disassociation and cellulose depolymerization (Koz and Cevik, 2014). The following oxidation of acid-pretreated lignocellulose from mixed-chemicals (NaOH, H_2O_2)

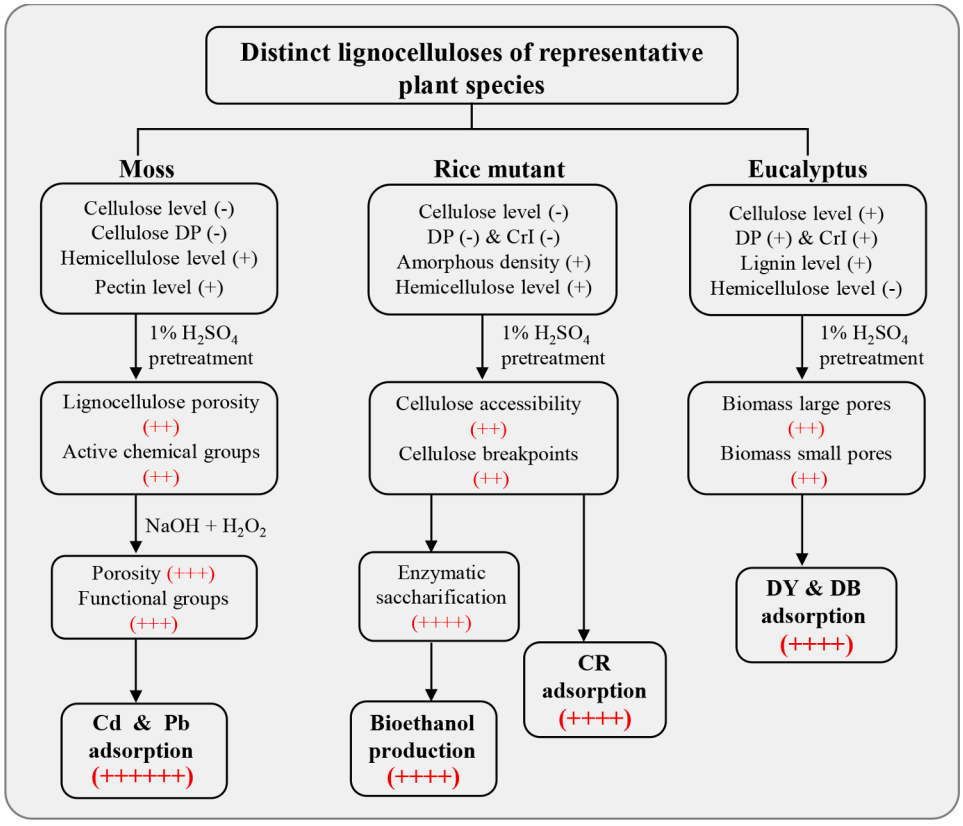

Fig. 6. A mechanism model about distinct lignocelluloses of three representative plant species selective for either complete biomass enzymatic saccharification towards high bioethanol production or desirable biosorbent assembly applicable for maximizing two heavy metals (Cd, Pb) and three diverse dyes (Congo-red (CR), direct-yellow (DY) and direct-blue (DB)) adsorption capacities. (+) & (−) in black highlighted as raised and reduced major factor of lignocellulose, respectively; (+) in red as upgrading scale for high-yield biomass saccharification and high-performance biosorbent assembly.

incubation causes a regular grain-like biosorbent assembly upgrading multiple-layer porosity and functional chemical groups (Mahmood-ul-Hassan et al., 2015), which simultaneously enables physical and chemical interactions with heavy metals to achieve the maximum adsorption capacity (Fig. 5B). Since several rice site-mutants of OsCESAs are identified for reduced cellulose level and recalcitrant factors such as cellulose CrI and DP (Hu et al., 2023), it has been also characterized that the length-reduced cellulose nanofibrils of rice mutants are assembled by increasing amorphous chains as breakpoints for initiation and completion of cellulose digestion into fermentable glucose for high bioethanol production (Zhang et al., 2023). As acid pretreatment could effectively digest amorphous cellulose chains and partial hemicellulose, it thus explains why the acid-pretreated lignocellulose of rice mutant is of remarkably upgraded cellulose accessibility for either complete biomass enzymatic saccharification or much higher CR adsorption capacity examined (Figs. 2, 3C). However, as eucalyptus plant contains relatively low proportion of hemicellulose, the 1% H_2SO_4 pretreatment should effectively create diverse large and small pores of lignocellulose by mostly digesting its hemicellulose linked between cellulose microfibrils and lignin, which results in the highest DY and DB adsorption capacities examined in this study (Fig. 3D). Therefore, this hypothetic model has sorted out how each representative plant species could provide its unique lignocellulose substrate selective for complete biomass saccharification and the optimal biosorbent assembly.

4. Conclusion

By selecting 15 plant species representing plant evolution from lower to higher plants, this study examined distinct lignocelluloses for diverse biomass enzymatic saccharification. The rice mutant is of near-complete cellulose hydrolysis and upgraded cellulose accessibility, interpreting how bioethanol productivity and Congo-red adsorption capacity are remarkably elevated. Performing oxidative catalysis with lignocelluloses, the optimal moss biosorbent is assembled for the maximum adsorptions with heavy metals, whereas the eucalyptus biosorbent has the highest adsorptions with organic dyes. A novel strategy is proposed to elucidate how characteristic lignocelluloses of plant evolution are convertible and selective for high-yield bioethanol and high-performance biosorbents.

CRediT authorship contribution statement

Huiyi Zhang: Writing – original draft, Methodology, Investigation, Formal analysis. **Yongtai Wang:** Writing – review & editing, Investigation, Formal analysis. **Hao Peng:** Methodology, Investigation, Formal analysis. **Boyang He:** Methodology, Investigation, Formal analysis. **Yunong Li:** Methodology, Investigation, Formal analysis. **Hailang Wang:** Methodology, Investigation, Formal analysis. **Zhen Hu:** Validation, Supervision, Funding acquisition. **Hua Yu:** Methodology, Investigation, Formal analysis. **Yanting Wang:** Validation, Supervision, Funding acquisition. **Mengzhou Zhou:** Validation, Supervision, Funding acquisition. **Liangcai Peng:** Validation, Supervision, Funding acquisition. **Miao Wang:** Writing – review & editing, Supervision, Methodology, Conceptualization.

Declaration of competing interest

The authors declare that they have no known competing financial interests or personal relationships that could have appeared to influence the work reported in this paper.

Acknowledgments

This work was in part supported by the National Natural Science Foundation of China (32470273, 32400212, 32170268, 32101701), the National 111 Project of the Ministry of Education of China (BP0820035, D17009), and the Initiative Grant of Hubei University of Technology for High-level Talents (GCC20230001).

Appendix A. Supplementary data

Supplementary data to this article can be found online at https://doi.org/10.1016/j.biortech.2024.131856.

Data availability

Data will be made available on request.

References

Abdolali, A., Ngo, H.H., Guo, W., Zhou, J.L., Zhang, J., Liang, S., Chang, S.W., Nguyen, D. D., Liu, Y., 2017. Application of a breakthrough biosorbent for removing heavy metals from synthetic and real wastewaters in a lab-scale continuous fixed-bed column. Bioresour. Technol. 229, 78–87.

Ai, Y., Wang, H., Liu, P., Yu, H., Sun, M., Zhang, R., Tang, J., Wang, Y., Feng, S., Peng, L., 2024. Insights into contrastive cellulose nanofibrils assembly and nanocrystals catalysis from dual regulations of plant cell walls. Sci. Bull. S2095-9273(24)00409-2. Advance online publication. Doi: 10.1016/j.scib.2024.06.013.

Çelebi, H., 2020. Recovery of detox tea wastes: usage as a lignocellulosic adsorbent in Cr^{6+} adsorption. J. Environ. Chem. Eng. 8 (5), 104310.

Cosgrove, D.J., 2024. Structure and growth of plant cell walls. Nat. Rev. Mol. Cell Biol. 25 (5), 340–358.

Dubey, S., Shri, M., Gupta, A., Rani, V., Chakrabarty, D., 2018. Toxicity and detoxification of heavy metals during plant growth and metabolism. Environ. Chem. Lett. 16, 1169–1192.

Fan, C., Zhang, W., Guo, Y., Sun, K., Wang, L., Luo, K., 2022. Overexpression of PtoMYB115 improves lignocellulose recalcitrance to enhance biomass digestibility and bioethanol yield by specifically regulating lignin biosynthesis in transgenic poplar. Biotechnol. Biofuels. Bioprod. 15 (1), 119.

González-Feijoo, R., Santás-Miguel, V., Arenas-Lago, D., Álvarez-Rodríguez, E., Núñez-Delgado, A., Arias-Estévez, M., Pérez-Rodríguez, P., 2024. Effectiveness of cork and pine bark powders as biosorbents for potentially toxic elements present in aqueous solution. Environ. Res. 250, 118455.

Gu, Y., Guo, J., Nawaz, A., Ul Haq, I., Zhou, X., Xu, Y., 2021. Comprehensive investigation of multiples factors in sulfuric acid pretreatment on the enzymatic hydrolysis of waste straw cellulose. Bioresour. Technol. 340, 125740.

He, X., Hong, Z.N., Jiang, J., Dong, G., Liu, H., Xu, R.K., 2021. Enhancement of Cd (II) adsorption by rice straw biochar through oxidant and acid modifications. Environ. Sci. Pollut. 28, 42787–42797.

Hokkanen, S., Bhatnagar, A., Sillanpää, M., 2016. A review on modification methods to cellulose-based adsorbents to improve adsorption capacity. Water Res. 91, 156–173.

Hu, Z., Peng, H., Liu, J., Zhang, H., Li, S., Wang, H., Lv, Z., Wang, Y., Sun, D., Tang, J., Peng, l., Wang, Y, 2023. Integrating genetic-engineered cellulose nanofibrils of rice straw with mild chemical treatments for enhanced bioethanol conversion and bioaerogels production. Ind. Crops Prod. 202, 117044.

Huang, Q., Hu, D., Chen, M., Bao, C., Jin, X., 2019. Sequential removal of aniline and heavy metal ions by jute fiber biosorbents: a practical design of modifying adsorbent with reactive adsorbate. J. Mol. Liq. 285, 288–298.

Huang, C., Jiang, X., Shen, X., Hu, J., Tang, W., Wu, X., Ragauskas, A., Jameel, H., Meng, X., Yong, Q., 2022. Lignin-enzyme interaction: a roadblock for efficient enzymatic hydrolysis of lignocellulosics. Rnew. Sust. Energ. Rev. 154, 111822.

Koz, B., Cevik, U.Ğ.U.R., 2014. Lead adsorption capacity of some moss species used for heavy metal analysis. Ecol. Indic. 36, 491–494.

Kwok, T.T., Fogg, D.N., Realff, M.J., Bommarius, A.S., 2017. Applying direct yellow 11 to a modified Simons' staining assay. Cellulose 24 (6), 2367–2373.

Leu, S.Y., Zhu, J.Y., 2013. Substrate-related factors affecting enzymatic saccharification of lignocelluloses: our recent understanding. Bioenerg. Res. 6, 405–415.

Mahmood-ul-Hassan, M., Suthar, V., Rafique, E., Ahmad, R., Yasin, M., 2015. Kinetics of cadmium, chromium, and lead sorption onto chemically modified sugarcane bagasse and wheat straw. Environ. Monit. Assess 187, 470.

Meng, X., Wells, T., Sun, Q., Huang, F., Ragauskas, A., 2015. Insights into the effect of dilute acid, hot water or alkaline pretreatment on the cellulose accessible surface area and the overall porosity of Populus. Green Chem. 17 (8), 4239–4246.

Park, S., Song, J., Lee, W.C., Jang, S., Lee, J., Kim, J., Kim, H.-K., Min, K., 2023. Advances in biomass-derived electrode materials for energy storage and circular carbon economy. Chem. Eng. J. 470, 144234.

Ramrakhiani, L., Halder, A., Majumder, A., Mandal, A.K., Majumdar, S., Ghosh, S., 2017. Industrial waste derived biosorbent for toxic metal remediation: mechanism studies and spent biosorbent management. Chem. Eng. J. 308, 1048–1064.

Sabarish, R., Unnikrishnan, G., 2018. Polyvinyl alcohol/carboxymethyl cellulose/ZSM-5 zeolite biocomposite membranes for dye adsorption applications. Carbohydr. Polym. 199, 129–140.

Saman, N., Tan, J.W., Mohtar, S.S., Kong, H., Lye, J.W.P., Johari, K., Hassan, H., Mat, H., 2018. Selective biosorption of aurum (III) from aqueous solution using oil palm trunk (OPT) biosorbents: equilibrium, kinetic and mechanism analyses. Biochem. Eng. J. 136, 78–87.

Soltis, D.E., Bell, C.D., Kim, S., Soltis, P.S., 2008. Origin and early evolution of angiosperms. Ann. n. y. Acad. Sci. 1133 (1), 3–25.

Su, C., Cai, D., Zhang, H., Wu, Y., Jiang, Y., Liu, Y., Zhang, C., Li, C., Qin, P., Tan, T., 2024. Pilot-scale acetone-butanol-ethanol fermentation from corn stover. Green Carbon 2 (1), 81–93.
Sun, Z., Bottari, G., Afanasenko, A., Stuart, M.C., Deuss, P.J., Fridrich, B., Barta, K., 2018. Complete lignocellulose conversion with integrated catalyst recycling yielding valuable aromatics and fuels. Nat. Catal. 1 (1), 82–92.
Tan, X.Y., Nielsen, J., 2022. The integration of bio-catalysis and electrocatalysis to produce fuels and chemicals from carbon dioxide. Chem. Soc. Rev. 51 (11), 4763–4785.
Vo, T.S., Hossain, M.M., Jeong, H.M., Kim, K., 2020. Heavy metal removal applications using adsorptive membranes. Nano Convergence. 7, 36.
Wang, C., Mei, J., Zhang, L., 2021. High-added-value biomass-derived composites by chemically coupling post-consumer plastics with agricultural and forestry wastes. J. Clean. Prod. 284, 124768.
Wang, X.Q., Ran, J.H., 2014. Evolution and biogeography of gymnosperms. Mol. Phylogenet. Evol. 75, 24–40.
Wang, M., Wang, Y., Liu, J., Yu, H., Liu, P., Yang, Y., Sun, D., Kang, H., Wang, Y., Tang, J., Fu, C., Peng, L., 2024. Integration of advanced biotechnology for green carbon. Green Carbon 2, 164–175.
Wiman, M., Dienes, D., Hansen, M.A., van der Meulen, T., Zacchi, G., Lidén, G., 2012. Cellulose accessibility determines the rate of enzymatic hydrolysis of steam pretreated spruce. Bioresour. Technol. 126, 208–215.
Wu, J., Elliston, A., Le Gall, G., Colquhoun, I.J., Collins, S.R.A., Wood, I.P., Dicks, J., Roberts, I.N., Waldron, K.W., 2018. Optimising conditions for bioethanol production from rice husk and rice straw: effects of pre-treatment on liquor composition and fermentation inhibitors. Biotechnol. Biofuels 11, 62.
Wu, J., Dong, J., Wang, J., 2022. Adsorptive removal of Cu (II) from aqueous solution by fermented sweet sorghum residues as a novel biosorbent. J. Mol. Liq. 367, 120362.
Wu, L., Feng, S., Deng, J., Yu, B., Wang, Y., He, B., Peng, H., Li, Q., Hu, R., Peng, L., 2019. Altered carbon assimilation and cellulose accessibility to maximize bioethanol yield under low-cost biomass processing in corn brittle stalk. Green Chem. 21 (16), 4388–4399.
Yaashikaa, P.R., Kumar, P.S., Saravanan, A., Vo, D.V.N., 2021. Advances in biosorbents for removal of environmental pollutants: a review on pretreatment, removal mechanism and future outlook. J. Hazard. Mater. 420, 126596.
Yang, T., Wang, Y., Sheng, L., He, C., Sun, W., He, Q., 2020. Enhancing Cd (II) sorption by red mud with heat treatment: performance and mechanisms of sorption. J. Environ. Manage. 255 (1), 109866.
Yu, H., Xiao, W., Han, L., Huang, G., 2019. Characterization of mechanical pulverization/phosphoric acid pretreatment of corn stover for enzymatic hydrolysis. Bioresour. Technol. 282, 69–74.
Yuan, T., Zeng, J., Wang, B., Cheng, Z., Chen, K., 2021. Lignin containing cellulose nanofibers (LCNFs): lignin content-morphology-rheology relationships. Carbohydr. Polym. 254, 117441.
Zhang, R., Hu, Z., Wang, Y., Hu, H., Li, F., Li, M., Ragauskas, A., Xia, T., Han, H., Tang, J., Yu, H., Xu, B., Peng, L., 2023. Single-molecular insights into the breakpoint of cellulose nanofibers assembly during saccharification. Nat. Commun. 14 (1), 1100.
Zhang, F., Xu, L., Xu, F., Jiang, L., 2021. Different acid pretreatments at room temperature boost selective saccharification of lignocellulose via fast pyrolysis. Cellulose 28, 81–90.
Zoghlami, A., Paës, G., 2019. Lignocellulosic biomass: understanding recalcitrance and predicting hydrolysis. Front. Chem. 7, 874.